

Comprehensive picture of VO₂ from band theory

Zhiyong Zhu* and Udo Schwingenschlöggl†

Physical Sciences and Engineering Division, KAUST, Thuwal 23955-6900, Kingdom of Saudi Arabia

(Received 22 June 2012; published 28 August 2012)

The structural, electronic, and magnetic features of the metal-insulator transition from the tetragonal rutile (R) to the monoclinic ($M1$) phase of VO₂ are well reproduced by band theory using the modified Becke-Johnson exchange potential. Based on this description, we identify a tendency for monoclinic charge ordering in the R phase due to electronic correlations as the origin of the phase transition. Whereas, the structural changes are crucial for the gap opening in the $M1$ phase, spin degeneracy in both phases is stabilized by correlation-induced delocalization of the V $3d$ electrons.

DOI: [10.1103/PhysRevB.86.075149](https://doi.org/10.1103/PhysRevB.86.075149)

PACS number(s): 71.20.Be, 71.30.+h, 71.27.+a

I. INTRODUCTION

For many years, metal-insulator transitions (MITs) in correlated electron systems have received a great amount of attention owing to the rich concomitant physics,¹ such as the anomalous metallicity associated with quantum criticality.² A prototypical example is VO₂,³ which, upon cooling below 340 K, undergoes a transition from a high-temperature metallic rutile phase (R) to a low-temperature insulating monoclinic phase ($M1$) with a dimerization of the V atoms into pairs and a twisting of these pairs. Moreover, a MIT from the R into a second monoclinic insulating phase ($M2$) has been established in slightly Cr-doped VO₂ (Ref. 4) as well as pristine VO₂ under uniaxial pressure.⁵ In the $M2$ phase, half of the V chains along the rutile c axis develops V-V pairs but does not twist, whereas, the other half twists but does not pair. Besides the temperature, MITs in VO₂ systems can also be driven by pressure,⁶ light,⁷⁻⁹ electric field,¹⁰ and doping,¹¹ giving rise to an important benchmark problem for modern condensed-matter physics.

The magnetic properties prominently distinguish the $M1$ and $M2$ phases. Because of the antiferromagnetism in the latter, the R - $M2$ transition is identified to be of Mott-Hubbard type.¹² On the other hand, the nonmagnetic nature of the former complicates the understanding of the R - $M1$ transition, which is still puzzling after years of intensive research. An electron-correlation-driven Mott-Hubbard transition,^{13,14} a structure-driven Peierls transition,^{11,15,16} and the cooperation of both these mechanisms¹⁷⁻¹⁹ have been proposed. Each proposal is supported by various experimental and theoretical results. A way to tackle the MITs is to study the role of electron correlations through the transitions by first-principles calculations based on or going beyond density functional theory.²⁰⁻²⁹ So far, however, a consistent description of the different structural, electronic, and magnetic aspects of the MITs in VO₂ could not be reached.

In the following, we will address the long-standing problem of the nature of the R - $M1$ transition in VO₂ by all-electron *ab initio* calculations in the framework of density functional theory. The modified Becke-Johnson exchange potential turns out to be the key to a consistent description of the MIT. The role of electron correlations will be discussed in detail. We argue that the transition into the $M1$ phase is driven by electron correlations due to their orbital polarization effect.

II. METHODOLOGY

Full-potential linearized augmented plane-wave calculations are performed using the WIEN2K package.³⁰ The crystal structures used in the calculations are taken from the experiments.^{31,32} To exclude errors in the comparison of total energies, the R phase is modeled by a nonprimitive unit cell that is equivalent to the unit cell of the $M1$ phase, see the marked areas in Figs. 1(a) and 1(b). A threshold energy of -6.0 Ry is used to separate the valence from the core states. The same R_{mt} (1.72 bohr for V and 1.52 bohr for O), $R_{\text{mt}}K_{\text{max}} = 7$, $\ell_{\text{max}} = 10$, and \vec{k} mesh ($7 \times 7 \times 8$) are used in all calculations. Besides the local density approximation³³ (LDA) and generalized gradient approximation³⁴ (GGA) for the exchange-correlation potential, a semilocal combination of the modified Becke-Johnson exchange and LDA correlation potentials (mBJLDA)³⁵ is employed. The latter is expected to treat electron correlations with a similar accuracy as the computationally expensive GW and hybrid methods.

III. RESULTS AND DISCUSSION

Nonmagnetic (NM) calculations for the R and $M1$ phases using the LDA, GGA, and mBJLDA functionals lead to the band structures and electronic densities of states (DOS) shown in Figs. 2 and 3. In addition, spin-polarized calculations have been performed for ferromagnetic (FM) and antiferromagnetic (AFM) orderings of the V spins along the c axis. Relative energies with respect to the NM R phase are listed in Table I. For both the LDA and the GGA, we find: FM ordering is preferred in both the R and the $M1$ phases, the $M1$ phase is metallic, and a R - $M1$ transition is energetically not favorable as the total energy is higher for the NM $M1$ phase than for the NM R phase. All these results contradict experimental observations, according to which, the transition in VO₂ is a NM-to-NM MIT from the high temperature R to the low temperature $M1$ phase. Therefore, LDA and GGA calculations fail to explain the structural, electronic, and magnetic features of the MIT. However, these features are well reproduced by the mBJLDA approach: The R phase is correctly predicted as a NM metal with a higher energy than the NM-insulating $M1$ phase.

In past years, various theoretical approaches have been tested, attempting to uncover the physics of the MIT in VO₂. This includes the LDA/GGA (Ref. 20) and LDA + U (Refs. 22 and 23) methods dynamic mean-field theory (DMFT) and its

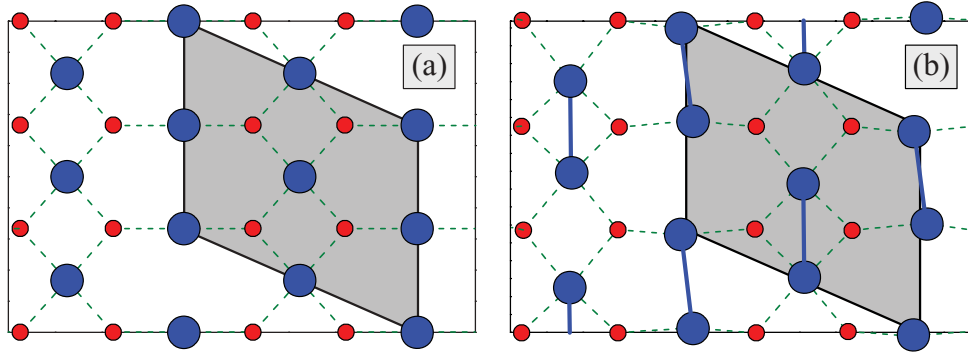


FIG. 1. (Color online) Atomic positions in the V-O plane in the (a) *R* and (b) *M1* phases. V and O atoms are indicated by large and small spheres, respectively.

variants,^{24,25,29} the *GW* method and its variants,^{21,26,27} and the hybrid functional method.²⁸ The merits and problems of these approaches in reproducing the MIT in VO₂ are summarized in Table II and are compared to the findings of the present paper. The LDA/GGA method fails miserably except for the metallic nature of the *R* phase. The LDA + *U* method finds insulating AFM states for both phases where only the insulating state of the *M1* phase is correct. Although the DMFT and its variants can predict the metallic and insulating states of the *R* and *M1* phases, respectively, they are based on adjustable parameters. The *GW* method can predict the electronic features of the MIT only if the parameter-based model variant is employed or self-consistent quasiparticle calculations are performed on the Coulomb-hole and screened-exchange (COHSEX) level. Moreover, the hybrid Heyd-Scuseria-Ernzerhof (HSE) method reproduces the metallic and insulating states of the *R* and *M1* phases, respectively, but not the magnetic properties.

In contrast to the previous methods, Table I shows that mBJLDA calculations reproduce all the structural, electronic, and magnetic features of the MIT. The mBJLDA method of density functional theory, therefore, enables a full band-theory explanation of the MIT in VO₂ despite strong electron correlations. The reasons for this success are that the approach

mimics the behavior of orbital-dependent potentials, thus, going beyond the LDA/GGA method and that correlation effects are treated not only for localized (as in the LDA + *U* method), but also for delocalized electrons.

As the failure of the LDA/GGA and success of the mBJLDA can be attributed to different descriptions of the electron correlations,³⁵ the role of electron correlations for the MIT in VO₂ can be extracted from a comparison of these two schemes. We calculate the V 3*d* charge density distribution in the energy range of $E_F - 1.0 \text{ eV} < E < E_F$ for the *R* phase and show the results in Fig. 4. The representation refers to the V-O plane as defined in Fig. 1(a). The LDA [Fig. 4(a)] and GGA (not shown) charge density distributions maintain the symmetry of the underlying crystal structure. In the mBJLDA results [Fig. 4(b)], however, a charge redistribution in every other V chain breaks the horizontal and vertical mirror symmetries. This charge redistribution can be attributed to the orbital polarization effect of electron correlations,³⁶ which is captured by the orbital-dependent potentials of the mBJLDA. Further analysis shows that the redistributed charge density reflects the lower symmetry of the *M1* phase (space group *P2₁/c*) as indicated by the black solid lines in Fig. 4(b). This tells us that a correlation-driven charge ordering with reduced symmetry is

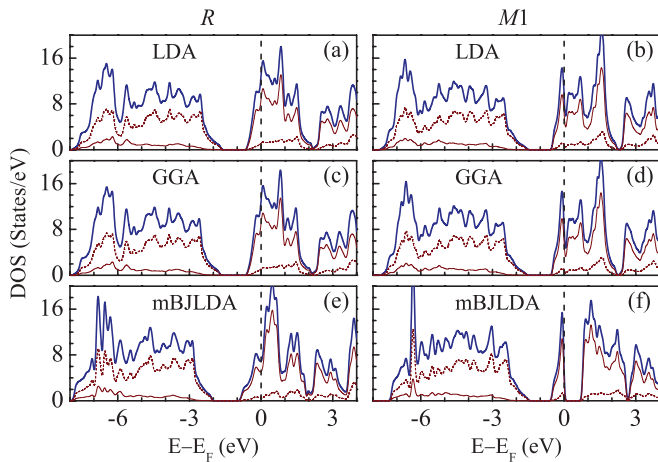


FIG. 2. (Color online) DOS of the (a), (c), and (e) *R* and (b), (d), and (f) *M1* phases of VO₂ obtained by (a) and (b) LDA, (c) and (d) GGA, and (e) and (f) mBJLDA calculations. The total DOS is indicated by thick solid lines, whereas, thin solid and dashed lines represent the partial V 3*d* and O 2*p* DOS.

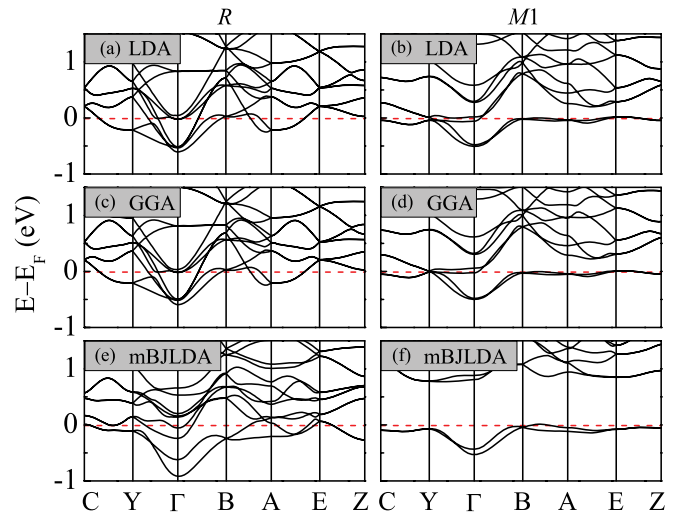


FIG. 3. (Color online) Electronic band structures of the (a), (c), and (e) *R* and (b), (d), and (f) *M1* phases of VO₂ obtained by (a) and (b) LDA, (c) and (d) GGA, and (e) and (f) mBJLDA calculations.

TABLE I. Relative energies (meV per VO₂) of the *R* and *M1* phases of VO₂ in different magnetic configurations with respect to the nonmagnetic *R* phase. NM, FM, and AFM orderings of the V spins along the *c* axis are addressed. The electron correlations are treated on the following levels of approximation: LDA, GGA, and mBJLDA.

	<i>R</i>			<i>M1</i>		
	NM	FM	AFM	NM	FM	AFM
LDA	0	-38.4	0	49.3	47.7	49.3
GGA	0	-101.2	-12.7	29.4	-10.6	27.5
mBJLDA	0	490.3	439.5	-96.3	629.7	377.8

favorable in the *R* structure at $T = 0$. Therefore, the structural change at the *R*-*M1* transition is only a secondary effect in response to charge ordering, i.e., of purely electronic nature. Note that the temperature counteracts the intrinsic tendency for charge ordering.

We notice that the charge ordering exhibits only half the periodicity of the *M1* structure. That is, additional structural changes that double the periodicity along the V chains (V dimerization and twisting of V pairs) are required to fully resemble the experimental situation. Regarding the driving force behind the periodicity doubling, two alternative scenarios come to mind: The first is a structure-driven Peierls picture. However, this scenario can be excluded because of the wrong energy hierarchy of the *R* and *M1* phases predicted by plain LDA/GGA calculations, see Table I. On the other hand, the stabilization of the *M1* phase against the *R* phase in the mBJLDA calculations points again to effects of electron correlations. The reason for this is that the structural changes result in an orbital polarization, which gives an energy gain in the mBJLDA (due to the orbital-dependent potentials).³⁷

Even in the presence of charge ordering, the *R* phase is metallic, see Figs. 2(e) and 3(e). Only after the structural transition into the *M1* phase is an insulating ground state formed, see Figs. 2(f) and 3(f). This indicates that the structural changes are necessary for opening the band gap. Indeed, a strong localization of the V *3d* electrons is observed at the *R*-*M1* transition, see the significant band flattening near E_F from the *R* to the *M1* phase shown in Fig. 3. On the other hand, the enhanced electron-electron interaction due to the localization is better described by the mBJLDA than by the LDA/GGA. Accordingly, a band gap is opened in the *M1* phase only in the former case, see Figs. 2(f) and 3(f). In this sense,

TABLE II. Merits and problems of different theoretical approaches in reproducing the MIT in VO₂. Criteria: (1) The total energy of the nonmagnetic *M1* phase is lower than that of the nonmagnetic *R* phase. (2) The *R* phase shows no long-range magnetic order. (3) The *M1* phase is nonmagnetic. (4) The *R* phase is metallic. (5) The *M1* phase is insulating. Fulfilled and not fulfilled criteria are shown by \checkmark 's and \times 's, respectively ($-$ indicates that the criterion is not considered in the reference).

	Criteria					Reference
	(1)	(2)	(3)	(4)	(5)	
LDA	\checkmark	-	-	\checkmark	\times	20
LDA/GGA	\times	\times	\times	\checkmark	\times	Present paper
LDA + U	-	\times	\times	\times	\checkmark	22 and 23
DMFT	-	-	-	\checkmark	\checkmark	25
DMFT + V	-	-	-	-	\checkmark	29
Cluster DMFT	-	-	-	\checkmark	\checkmark	24
Model <i>GW</i>	-	-	-	-	\checkmark	21
<i>GW</i>	-	-	-	\checkmark	\times	27
LDA + G_0W_0	-	-	-	\checkmark	\times	26
COHSEX + G_0W_0	-	-	-	\checkmark	\checkmark	26
HSE	-	-	-	\checkmark	\checkmark	28
mBJLDA	\checkmark	\checkmark	\checkmark	\checkmark	\checkmark	Present paper

both electron correlations and the induced structural changes are needed for the *M1* phase to be insulating.

In both *R* and *M1* phases, the V atoms show no spin polarization for the mBJLDA, whereas, local magnetic moments are stabilized for the LDA/GGA. This observation can be attributed to a delocalization of the V *3d* electrons due to electron correlations as indicated by the DOS in Fig. 2 and band structures in Fig. 3. In the *R* phase, the electron correlations widen the V *3d* band from ~ 0.5 eV (LDA/GGA) to ~ 1.0 eV (mBJLDA), whereas, in the *M1* phase, this widening is less significant. However, an enhanced dispersion of the V *3d* bands is still evident in the mBJLDA results for the *M1* phase (Fig. 3), for example, along path B-A. Spin splitting of less localized V *3d* electrons costs more kinetic energy and, therefore, results in NM *R* and *M1* phases.

IV. CONCLUSION

In conclusion, band theory can provide a comprehensive picture of all structural, magnetic, and electronic features of the prototypical metal-insulator transition in VO₂ in agreement with the experimental situation. This description enables us

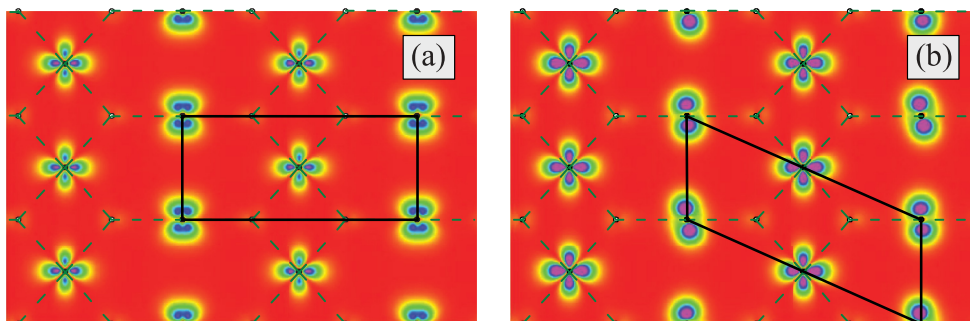


FIG. 4. (Color online) V *3d* charge density distributions in the V-O plane obtained for the *R* phase by (a) LDA and (b) mBJLDA calculations.

to answer the long-standing question about the origin of the R - $M1$ phase transition: The failure of the LDA/GGA method in predicting the correct energy hierarchy of the R and $M1$ phases excludes a structure-driven Peierls scenario. On the other hand, stabilization of the $M1$ against the R phase by the mBJLDA method indicates that the structural changes in the $M1$ phase are correlation assisted by the orbital polarization effect. In addition, in both phases, spin degeneracy is stabilized by a correlation-driven delocalization of the V $3d$ electrons, whereas, both electron correlations and structural changes are required for the $M1$ phase to become insulating. Most importantly, already in high temperature R , structure

correlations induce a tendency for charge ordering with an intended order pattern that reflects the lower symmetry of the $M1$ phase, which is the origin of the R - $M1$ phase transition. As a consequence, the structural changes at the transition are only a secondary effect in response to a purely electronic mechanism. Our findings strongly indicate that the MIT in VO_2 should be characterized as a correlation-driven transition.

ACKNOWLEDGMENT

Fruitful discussions with H. Wang are gratefully acknowledged.

*zhiyong.zhu@kaust.edu.sa

†udo.schwingschlogl@kaust.edu.sa

- ¹M. Imada, A. Fujimori, and Y. Tokura, *Rev. Mod. Phys.* **70**, 1039 (1998).
- ²T. Misawa and M. Imada, *Phys. Rev. B* **75**, 115121 (2007).
- ³F. J. Morin, *Phys. Rev. Lett.* **3**, 34 (1959).
- ⁴J. P. Pouget, H. Launois, T. M. Rice, P. Dernier, A. Gossard, G. Villeneuve, and P. Hagenmuller, *Phys. Rev. B* **10**, 1801 (1974).
- ⁵J. P. Pouget, H. Launois, J. P. D'Haenens, P. Merenda, and T. M. Rice, *Phys. Rev. Lett.* **35**, 873 (1975).
- ⁶E. Arcangeletti, L. Baldassarre, D. Di Castro, S. Lupi, L. Malavasi, C. Marini, A. Perucchi, and P. Postorino, *Phys. Rev. Lett.* **98**, 196406 (2007).
- ⁷A. Cavalleri, C. Tóth, C. W. Siders, J. A. Squier, F. Rákai, P. Forget, and J. C. Kieffer, *Phys. Rev. Lett.* **87**, 237401 (2001).
- ⁸C. Kübler, H. Ehrke, R. Huber, R. Lopez, A. Halabica, R. F. Haglund, and A. Leitenstorfer, *Phys. Rev. Lett.* **99**, 116401 (2007).
- ⁹D. J. Hilton, R. P. Prasankumar, S. Fourmaux, A. Cavalleri, D. Brassard, M. A. El Khakani, J. C. Kieffer, A. J. Taylor, and R. D. Averitt, *Phys. Rev. Lett.* **99**, 226401 (2007).
- ¹⁰B. Wu, A. Zimmers, H. Aubin, R. Ghosh, Y. Liu, and R. Lopez, *Phys. Rev. B* **84**, 241410 (2011).
- ¹¹J. M. Booth and P. S. Casey, *Phys. Rev. Lett.* **103**, 086402 (2009).
- ¹²T. M. Rice, H. Launois, and J. P. Pouget, *Phys. Rev. Lett.* **73**, 3042 (1994).
- ¹³H.-T. Kim, Y. W. Lee, B.-J. Kim, B.-G. Chae, S. J. Yun, K.-Y. Kang, K.-J. Han, K.-J. Yee, and Y.-S. Lim, *Phys. Rev. Lett.* **97**, 266401 (2006).
- ¹⁴M. M. Qazilbash, M. Brehm, B.-G. Chae, P.-C. Ho, G. O. Andreev, B.-J. Kim, S. J. Yun, A. V. Balatsky, M. B. Maple, F. Keilmann, H. T. Kim, and D. N. Basov, *Science* **318**, 1750 (2007).
- ¹⁵J. B. Goodenough, *J. Solid State Chem.* **3**, 490 (1971).
- ¹⁶A. Cavalleri, T. Dekorsy, H. H. W. Chong, J. C. Kieffer, and R. W. Schoenlein, *Phys. Rev. B* **70**, 161102 (2004).
- ¹⁷K. Okazaki, H. Wadati, A. Fujimori, M. Onoda, Y. Muraoka, and Z. Hiroi, *Phys. Rev. B* **69**, 165104 (2004).
- ¹⁸T. C. Koethe, Z. Hu, M. W. Haverkort, C. Schüßler-Langeheine, F. Venturini, N. B. Brookes, O. Tjernberg, W. Reichelt, H. H. Hsieh, H.-J. Lin, C.-T. Chen, and L.-H. Tjeng, *Phys. Rev. Lett.* **97**, 116402 (2006).
- ¹⁹T. Yao, X. D. Zhang, Z. H. Sun, S. J. Liu, Y. Y. Huang, Y. Xie, C. Z. Wu, X. Yuan, W. Q. Zhang, Z. Y. Wu, G. Q. Pan, F. C. Hu, L. H. Wu, Q. H. Liu, and S. Q. Wei, *Phys. Rev. Lett.* **105**, 226405 (2010).
- ²⁰R. M. Wentzcovitch, W. W. Schulz, and P. B. Allen, *Phys. Rev. Lett.* **72**, 3389 (1994); **73**, 3043 (1994).
- ²¹A. Continenza, S. Massidda, and M. Posternak, *Phys. Rev. B* **60**, 15699 (1999).
- ²²M. A. Korotin, N. A. Skorikov, and V. I. Anisimov, *Phys. Met. Metallogr.* **94**, 17 (2002).
- ²³A. Liebsch, H. Ishida, and G. Bihlmayer, *Phys. Rev. B* **71**, 085109 (2005).
- ²⁴S. Biermann, A. Poteryaev, A. I. Lichtenstein, and A. Georges, *Phys. Rev. Lett.* **94**, 026404 (2005).
- ²⁵M. S. Laad, L. Craco, and E. Müller-Hartmann, *Phys. Rev. B* **73**, 195120 (2006).
- ²⁶M. Gatti, F. Bruneval, V. Olevano, and L. Reining, *Phys. Rev. Lett.* **99**, 266402 (2007).
- ²⁷R. Sakuma, T. Miyake, and F. Aryasetiawan, *Phys. Rev. B* **78**, 075106 (2008).
- ²⁸V. Eyert, *Phys. Rev. Lett.* **107**, 016401 (2011).
- ²⁹A. S. Belozarov, M. A. Korotin, V. I. Anisimov, and A. I. Poteryaev, *Phys. Rev. B* **85**, 045109 (2012).
- ³⁰P. Blaha, K. Schwarz, G. K. H. Madsen, D. Kvasnicka, and L. Luitz, WIEN2K, An augmented plane-wave + local orbitals program for calculating crystal properties (Technical University of Vienna, Vienna, 2001).
- ³¹D. B. McWhan, M. Marezio, J. P. Remeika, and P. D. Dernier, *Phys. Rev. B* **10**, 490 (1974).
- ³²J. M. Longo and P. Kierkegaard, *Acta Chim. Scand.* **24**, 420 (1970).
- ³³J. P. Perdew and Y. Wang, *Phys. Rev. B* **45**, 13244 (1992).
- ³⁴J. P. Perdew, K. Burke, and M. Ernzerhof, *Phys. Rev. Lett.* **77**, 3865 (1996).
- ³⁵F. Tran and P. Blaha, *Phys. Rev. Lett.* **102**, 226401 (2009).
- ³⁶A. I. Liechtenstein, V. I. Anisimov, and J. Zaanen, *Phys. Rev. B* **52**, R5467 (1995).
- ³⁷Z. Y. Zhu, X. H. Wang, and U. Schwingenschlögl, *Appl. Phys. Lett.* **98**, 241902 (2011).